Available online at www.sciencedirect.com
SCIENCE DIRECT®
Thermochimica Acta 431 (2005) 188–194
thermochimica acta
www.elsevier.com/locate/tca

Unilamellar vesicle-forming property of *N*-nervonoylsphingomyelin (C24:1-SM) as studied by differential scanning calorimetry and negative stain electron microscopy

Y. Kawasaki, H. Nishikido, A. Kuboki, S. Ohira, M. Kodama *

Department of Biochemistry, Faculty of Science, Okayama University of Science, 1-1 Ridai-cho, Okayama 700 0005, Japan

Received 12 November 2004; received in revised form 17 February 2005; accepted 21 February 2005
Available online 24 March 2005

Abstract

Focusing on an amide-linked fatty acid composition of naturally occurring sphingomyelins (SMs), *N*-palmitoylSM (C16:0-SM), *N*-stearoylSM (C18:0-SM), and *N*-nervonoylSM (C24:1-SM) were partially synthesized, respectively. The effect of C24:1-SM on the thermotropic behavior of respective vesicles of the C16:0-, and C18:0-SMs was investigated by a differential scanning microcalorimetry (DSC), and the structure of these semisynthetic SM vesicles was examined by a negative stain electron microscopy. Two vesicles of the saturated C16:0-SM and C18:0-SM showed sharp transition peaks at temperatures of 39.6 and 43.7 °C, respectively, in contrast with a broad and low-temperature transition peak observed for the unsaturated C24:1-SM vesicle. An electron micrograph of the C24:1-SM showed unilamellar vesicles of relatively small size (100–500 nm in diameter), in contrast to large multilamellar vesicles up to 3.5 μm in diameter observed for the C16:0-, and C18:0-SMs. This result indicated a unilamellar vesicle-forming property for the C24:1-SM. In this accord, a micrograph of sonicated vesicles of the C24:1-SM also showed unilamellar vesicles of regular size (∼100 nm), suggesting that the unilamellar vesicle is a thermodynamically stable state for the unsaturated C24:1-SM. Furthermore, when the C24:1-SM was added to the respective vesicles of C16:0-, and C18:0-SMs, both a broadening and a temperature-lowering for the transition peaks of these vesicles proceeded more and more with increasing the content of C24:1-SM. This was accounted for by a decrease in the multiplicity of the saturated SM vesicles caused by the unilamellar vesicle-forming property of the unsaturated SM.

Keywords: Semisynthetic sphingomyelins; Naturally occurring sphingomyelins; Differential scanning calorimetry (DSC); Electron microscopy

1. Introduction

Phospholipids are major components of biomembranes and are present in two types, glycerolipid and sphingolipid, depending on whether their backbone moiety is a glycerol or a sphingosine [1]. Accordingly, two chains of the sphingolipid differ in a functional group, thus, one is a sphingosine chain having hydroxyl (–OH) and amino groups (–NH) and the other is a fatty acid chain having a carbonyl group (–C=O). In this contrast, two chains of the glycerolipid are all fatty acids. A sphingomyelin (SM) with a phosphorylcholine headgroup is the most typical sphingolipid but it is a minor lipid constituent in biomembranes. However, much attention has been paid to the SMs since a new concept of lipid microdomains and/or lipid rafts was proposed [2–5]. This is because the SM molecules are critical participants in forming the specific lipid structure in biomembranes.

On the other hand, previous studies on naturally occurring SMs have revealed that there is a fair difference in the length of their fatty acid chain, thus, ranging from 14 to at least 24 carbons, in contrast to mostly the same length (18 carbons) for the other sphingosine chain [6–12]. Furthermore, it has been reported that the fatty acid composition of naturally occurring SMs significantly differs when they are obtained from different sources [9–11]. Surprisingly, such a fatty acid

* Corresponding author. Fax: +81 86 255 7700.
E-mail address: kodama@dbc.ous.ac.jp (M. Kodama).

0040-6031/$ – see front matter © 2005 Elsevier B.V. All rights reserved.
doi:10.1016/j.tca.2005.02.025

composition difference has been reported even for the same source of bovine brain SMs which are obtained from different suppliers [7–12]. However, the typical fatty acids of naturally occurring SMs are a saturated palmitic (C16:0) and stearic (C18:0) acids and an unsaturated nervonic (C24:1) acid which has a *cis* double bond at C-15 position [7–12]. These fatty acids compete in composition with one another. In this regard, it has been also reported that the thermotropic behavior of the gel-to-liquid crystal phase transition of the naturally occurring SMs depends predominantly on the content of norvonic acid [8–12] ranging from 5 to 70 mol% in a maximum. However, to date, a study on the *N*-nervonoylSM (C24:1-SM) is very scarce [13].

From this viewpoint, in the present study, the *N*-palmitoylSM (C16:0-SM), *N*-stearoylSM (C18:0-SM), and C24:1-SM were partially synthesized according to a procedure developed by Sripada et al. [14]. A number of studies have been reported with partially synthesized SMs [11,13–18]. So, for comparison with these studies, we chose the partial synthetic procedure. The effect of C24:1-SM on the phase transition behavior of respective vesicles composed of the C16:0-SM and C18:0-SM was investigated by a differential scanning microcalorimetry (DSC) and furthermore, a negative stain electron microscopy was performed to obtain structural information of sonicated and unsonicated vesicles of these semisynthetic SMs.

2. Experimental

2.1. Materials

2.1.1. Bovine brain SM (BSM)

Two BSMs (Lot Nos. 120K1580, 122K0367) obtained from different batches were purchased from Sigma Co. (St. Louis, MO). The fatty acid composition of two BSMs was obtained by a positive ion electrospray ionization mass spectrometry (ESI/MS) described below.

2.1.2. N-palmitoylSM (C16:0-SM), N-stearoylSM (C18:0-SM), and N-nervonoylSM (C24:1-SM)

C16:0-SM, C18:0-SM, and C24:1-SM were partially synthesized by deacylation–reacylation of the BSM according to a method previously reported by Sripada et al. [14]. The deacylation procedures are as follows: the BSM (∼500 mg) was dispersed in ∼35 ml of 1N methanolic HCl. The dispersion was stirred at a temperature around 70 °C for a period of 20 h and the solvent was then removed by a rotary evaporation. The resultant precipitates were suspended in benzene and the suspension was evaporated by rotary evaporating at least three times, subsequently followed by a silicic acid column chromatography (chloroform/methanol). The eluted fractions were monitored by a thin-layer chromatography developed in chloroform/methanol/ammonium hydroxide 25:17:3 (v/v/v). The product, sphingosylphosphocholine (SPC)·HCl, was dissolved in dry chloroform and was then neutralized by passing over negative ion exchange resin (Rexyn I-300). For the resultant SPC, the composition of sphingosine chains was examined with the ESI/MS and ^{13}C NMR and ^{1}H NMR spectroscopies, showing that more than 95% of the total chains were 18 carbons with a trans double bond at the C-4 position [14]. The reacylation procedures are as follows: the SPC dissolved in dry chloroform was reacylated with three fatty acids of saturated C16:0 and C18:0, and monounsaturated C24:1 in the presence of dicyclohexylcarbodiimide (DCC), respectively. Three final products, C16:0-SM, C18:0-SM, and C24:1-SM, were purified by the silicic acid column chromatography developed in chloroform/methanol changing in v/v from 9:1 to 1:7, respectively. The purification was repeated until a half height-width of the gel-to-liquid crystal phase transition peak for three semisynthetic SMs became the narrowest. The purity of three semisynthetic SMs was checked to be more than 95% by a combination of the thin-layer chromatography, NMR spectroscopy, and ESI/MS. However, as pointed out by other workers [14–18], some epimerization occurs at the C-3 position of sphingosine chain during the acid-deacylation procedures. This produces some of a L-*threo* stereoisomer of SPC. On this basis, the possibility of epimerization was checked for the three semisynthetic SMs by ^{13}C NMR and ^{1}H NMR spectroscopies. As a result, three respective semisynthetic SMs were found to be composed of 75% of the desired product D-*erythro* and 25% of the L-*threo* stereoisomer.

2.2. Preparation of vesicle dispersions

Dispersions of respective vesicles composed of the two naturally occurring BSMs and three semisynthetic SMs, C16:0-SM, C18:0-SM, and C24:1-SM, were prepared as follows [19]: a film of each lipid was first prepared by removing chloroform from the lipid stock solution on a rotary evaporator, and then under high vacuum (10^{-4} Pa) to achieve complete removal of traces of the solvent. The dried lipid film thus obtained was then dispersed in distilled water and gently vortexed at liquid crystal phase temperatures. Furthermore, a series of vesicle dispersions of the C16:0-SM containing 10, 30, 50, 70, and 90 mol% of the C24:1-SM was prepared from films of two lipid mixtures. The same procedure was applied to prepare a series of vesicle dispersions of the C18:0-SM containing the C24:1-SM.

2.3. Ultrasonic irradiation of vesicle dispersions

The vesicle dispersions of C16:0-SM, C18:0-SM, and C24:1-SM were ultrasonically irradiated by a bath sonicator equipped with a cap-horn sonifier (Branson Ultrasonic Co. Model 450), under a nitrogen atmosphere, at a power of 100 W for a period of 50 min, in a jacket vessel maintained at a desired liquid crystal phase temperature by a constant-temperature circulating water bath (Haake F3-C) [20].

Table 1
Fatty acid compositions of two naturally occurring BSMs obtained from Sigma Co.: BSM(a), Lot No.: 122K0367; BSM(b), Lot No.: 120K1580

CN:DBN[a] for amide-linked fatty acid chain	Composition (mol%)	
	BSM(a)	BSM(b)
14:0	0.7	0.0
14:1	2.0	0.0
16:0	47.0	3.3
16:2	2.1	0.0
17:0	1.4	0.0
18:0	11.0	39.4
19:0	0.0	0.7
20:0	2.8	6.0
20:2	2.9	0.0
21:0	0.0	1.3
22:0	1.5	2.0
22:1	2.2	0.0
23:0	4.2	2.7
24:0	17.6	12.4
24:1	4.7	31.5
24:2	0.0	0.8

[a] Total carbon number (CN):total double bond number (DBN) for amide-linked fatty acid chains estimated with a sphingosine chain C18:1.

2.4. Electrospray ionization mass spectrometry (ESI/MS) analysis for the fatty acid chains of naturally occurring BSMs

A fatty acid composition of two naturally occurring BSMs used in the present study was determined by ESI/MS performed with a JMS-LC mate instrument (JEOL, Japan) [6,7,12]. The mass of respective molecular species was determined with a positive ESI spectrum for a molecular ion adduct found as $[SM + Na]^+$ ($[SM + 23]^+$) and was then used to estimate both the total carbon number and the total double bond number for the sphingosine chain plus the amide-linked fatty acid chain of the respective molecular species. Subsequently, by assuming that all the sphingosine chains are C18:1, both the total carbon number and the total double bond number for the amide-linked fatty acid chain were calculated. Table 1 summarizes the total carbon number and the total double bond number obtained for the amide-linked fatty acid chain of the respective molecular species, together with their compositions, which are compared between two naturally occurring BSMs (a) (Lot No.: 122K0367) and (b) (Lot No.: 120K1580). The estimated average molecular weights are 741 and 772 for the BSM(a) and BSM(b), respectively.

2.5. Differential scanning calorimetry (DSC)

All calorimetric experiments were performed with a Microcal VP differential scanning microcalorimeter and on heating from 0 °C to temperatures of a liquid crystal phase at a rate of 45 °C h^{-1}. The lipid concentrations in the present DSC experiments were ~0.5 mM with a calorimetric cell volume of 0.52 ml. After the DSC, the lipid concentrations were estimated by a modified Bartlett phosphate assay [21].

2.6. Electron microscopy

Structural information of the lipid vesicles was obtained by a negative stain electron microscopy. A drop of the lipid vesicle dispersions (lipid concentration: ~2 mM) prepared according to a method described above (see Section 2.2) was placed on copper grids covered with carbon-coated collodion films, allowed to remain until becoming almost dry. A drop of 2% solution of sodium phosphotungstate (pH approximately 7) was added and the excess solution was then drained. After drying, the preparations were examined with a JEOL JEM-2000EX electron microscope operated at 200 kV.

3. Results and discussions

3.1. DSC

In Table 1, a fatty acid composition is compared between two naturally occurring BSMs (a) (Lot No.: 122K0367) and (b) (Lot No.: 120K1580) obtained from Sigma Co. In this table, we mark three fatty acids of C16:0, C18:0, and C24:1 which compete in composition with one another. Thus, the BSM(a) is abundant in C16:0, the content of which reaches approximately 47 mol%, whereas the BSM(b) is rich in C18:0 (approximately 39 mol%). Furthermore, a large amount of C24:1 (approximately 32 mol%) is observed for the BSM(b), in contrast with a small amount of C24:1 (approximately 5 mol%) for the BSM(a). In this accord, as shown in Fig. 1, the gel-to-liquid crystal phase transition behavior greatly differs between the two BSMs. The BSM(a) exhibits a relatively sharp transition peak with a maximum at approximately 35 °C, and estimated transition enthalpy is 33.9 kJ/mol lipid. In contrast, a broad peak characterized by two maxima at approximately 33 and 37 °C (ΔH = 33.0 kJ/mol lipid) is observed for the BSM(b). The thermodynamic parameters obtained for the two BSMs are summarized in Table 2.

For comparison with the naturally occurring BSMs shown in Fig. 1, Fig. 2 shows the gel-to-liquid phase transition behavior obtained for three semisynthetic SMs, C16:0-SM, C18:0-SM, and C24:1-SM. As shown in Fig. 2(a) and (b), both the C16:0-SM and C18:0-SM show single sharp transition peaks which appear, respectively, at midpoint temperatures of 39.6 and 43.7 °C. In this contrast, the C24:1-SM, shown in Fig. 2(c), exhibits a fairly broad and low-

Table 2
Thermodynamic parameters obtained for two naturally occurring BSMs and three semisynthetic SMs, C16:0-SM, C18:0-SM, and C24:1-SM

	T_m (°C)	ΔH (kJ/mol lipid)
BSM(a)	34.6	33.9
BSM(b)	32.9; 37.2	33.0
C16:0-SM	39.6	32.6
C18:0-SM	43.7	37.7
C24:1-SM	18.0; 22.3; 27.4	26.4

T_m is a temperature of transition peak maximum, and ΔH the gel-to-liquid crystal phase transition enthalpy per mole of lipid.

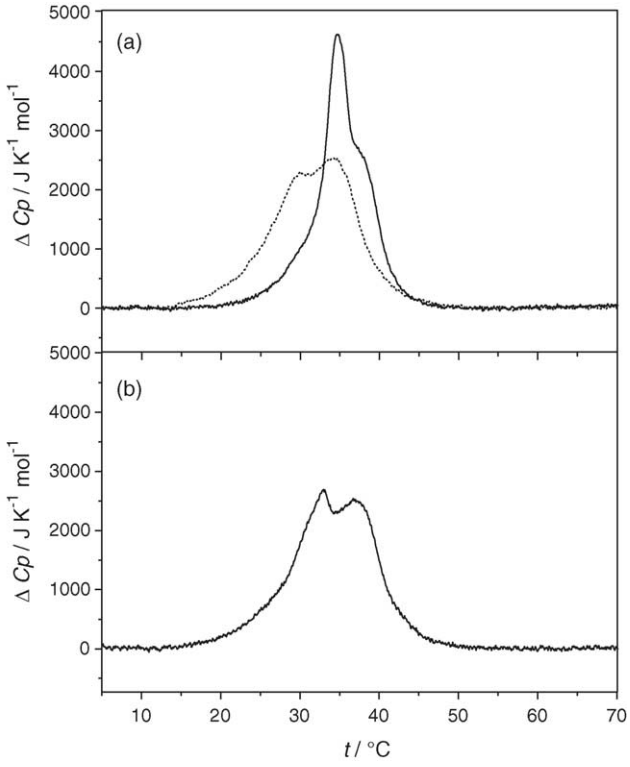

Fig. 1. The gel-to-liquid crystal phase transition behavior for naturally occurring BSMs obtained from Sigma Co.: (a) Lot No.: 122K0367; (b) Lot No.: 120K1580. Apparent excess heat capacity (ΔC_P) is plotted as a function of temperature (t). In this figure, the phase transition behavior of the BSM(a) containing the C24:1-SM added up to 30 mol% is shown by dotted lines.

temperature transition peak observed over temperatures of 10–35 °C. The thermodynamic parameters of three semisynthetic SMs are added to Table 2. In Table 2, a chain-length dependence of the gel-to-liquid crystal phase transition enthalpy is observed for the C16:0-SM and C18:0-SM [13,14]. However, the C24:1-SM having a *cis* double bond at the C-15 position shows a transition enthalpy (26.4 kJ/mol lipid) much smaller than expected from its acyl chain length (24 carbons). In fact, a saturated *N*-lignoceroylSM (C24:0-SM) shows a much larger transition enthalpy of 62.3 kJ/mol lipid (unpublished data obtained by us). This fact indicates that the chain packing of gel phase for the unsaturated C24:1-SM is fairly looser compared with that of the saturated *N*-acylSMs. Accordingly, the relatively broader and lower-temperature transition peak observed for the naturally occurring BSM(b), shown in Fig. 1, reveals a large contribution of the C24:1-SM which is contained up to 30 mol%. From this viewpoint, the C24:1-SM was added to the naturally occurring BSM(a) containing the less amount (5 mol%) of C24:1-SM. When the content of C24:1-SM added to the BSM(a) reached 30 mol%, the resultant transition peak (shown by dotted lines in Fig. 1(a)) became nearly the same in shape as that of BSM(b) shown in Fig. 1(b).

On the basis of these results, the effect of the C24:1-SM on the phase transition of both the synthetic C16:0-SM and C18:0-SM was investigated. In this experiment, the amount of C24:1-SM added to the respective vesicles of the C16:0-SM and C18:0-SM was changed from 10 to 90 mol%. In Fig. 3, the phase transition behavior of varying C24:1-SM contents is compared between the C16:0-SM (A) and C18:0-SM (B). As shown in Fig. 3A, a pronounced broadening of the transition peak of the C16:0-SM is observed at the C24:1-SM content of 10 mol% (b), above which the transition peak gradually becomes broader with increasing the content of C24:1-SM, simultaneously with a decrease in the transition temperature (c–f). As shown in Fig. 3A(c) and (d), doublet transition peaks are observed at the C24:1-SM contents of 30–50 mol%. In these content region, as shown in Fig. 4A, a significant decrease in the transition enthalpy is also observed. As shown in Figs. 3B and 4B, the effect of the C24:1-SM on the phase transition of the C18:0-SM vesicle was the same as that of the C16:0-SM vesicle.

3.2. Electron microscopy

The preparations of respective vesicles of C16:0-SM, C18:0-SM and C24:1-SM prepared according to a Bangham

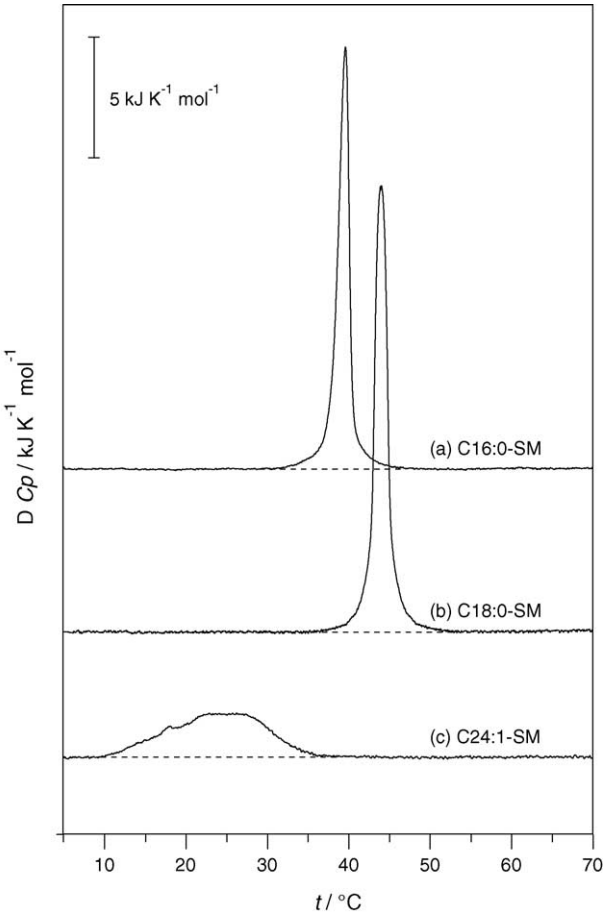

Fig. 2. The gel-to-liquid crystal phase transition behavior of (a) the saturated C16:0-SM and (b) C18:0-SM, and (c) the unsaturated C24:1-SM. Apparent excess heat capacity (ΔC_P) is plotted as a function of temperature (t).

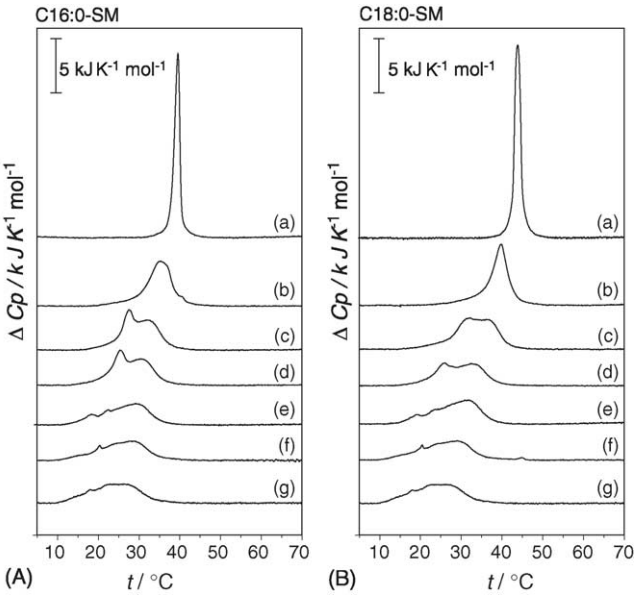

Fig. 3. Comparison of phase transition behavior between (A) the C16:0-SM and (B) C18:0-SM vesicles of varying C24:1-SM contents. Contents of the C24:1-SM (mol%): (a) 0; (b) 10; (c) 30; (d) 50; (e) 70; (f) 90; (g) 100.

method [19] were examined by a negative stain electron microscopy. Typical electron micrographs of these vesicles are compared in Fig. 5 for the C18:0-SM (a) and C24:1-SM (b). For the C18:0-SM shown in Fig. 5(a), multilamellar vesicles (MLVs) as large as 3.5 μm in diameter are observed, similarly to a result for the C16:0-SM (not shown data). In this contrast, the micrograph in Fig. 5(b) for the C24:1-SM shows unilamellar vesicles which are relatively irregular in size and range in diameter from 100 to 500 nm. When an ultrasonic irradiation was adopted for the dispersion of C24:1-SM vesicle, the resultant micrograph likewise exhibits unilamellar vesicles but their size is uniform (approximately ∼100 nm in diameter) as shown in Fig. 5(c), indicating that only a change

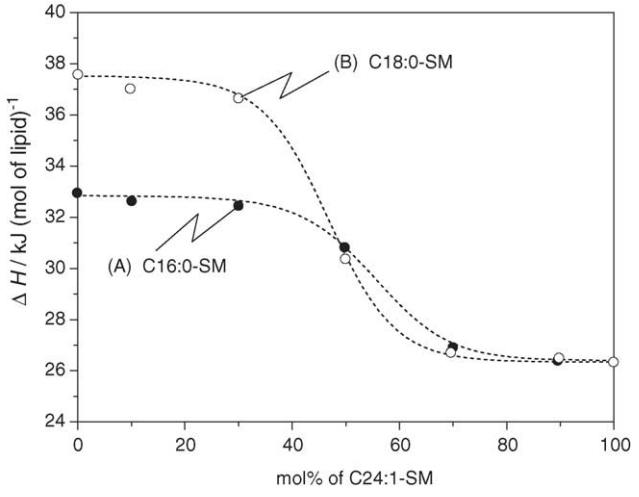

Fig. 4. Variation with increase in the C24:1-SM content (mol%) of phase transition enthalpy (ΔH) for respective vesicles of (A) the C16:0-SM and (B) the C18:0-SM.

in size occurs by the ultrasonic irradiation. In this accord, as shown in Fig. 6(a), the transition behavior of the sonicated vesicle of C24:1-SM is almost the same as that of its unsonicated vesicle. In this contrast, as shown in Fig. 6(b), the ultrasonic irradiation for the dispersion of C18:0-SM vesicle causes a significant broadening of the transition peak, simultaneously with a slight lowering of its temperature. In this connection, our previous study on sonicated vesicles of

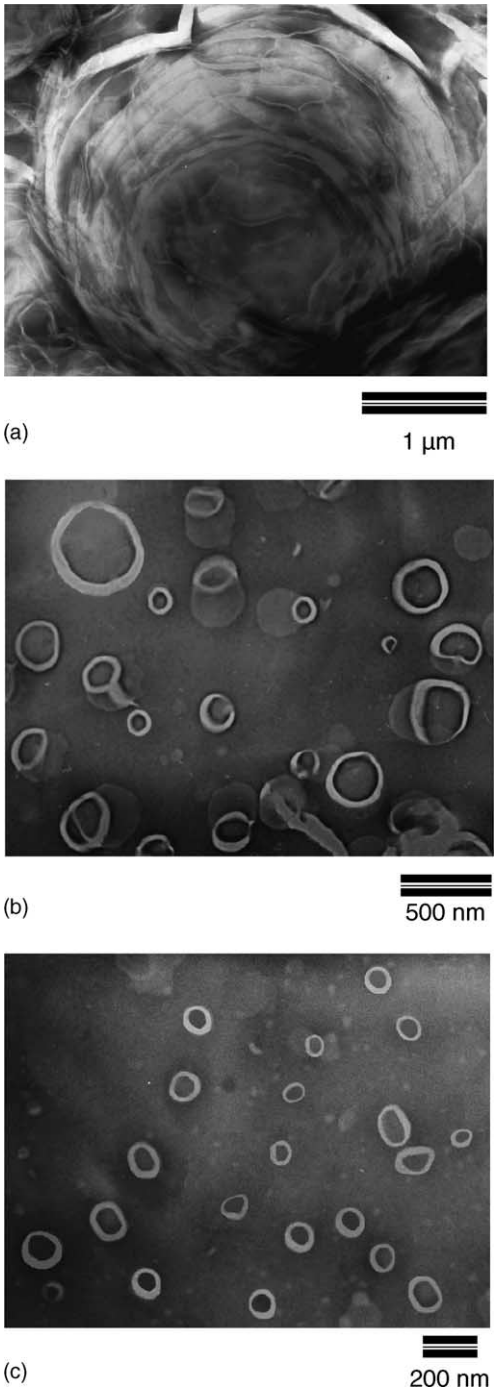

Fig. 5. Typical negative stain electron micrographs for the unsonicated vesicles of (a) C18:0-SM and (b) C24:1-SM, and (c) the sonicated vesicle of C24:1-SM.

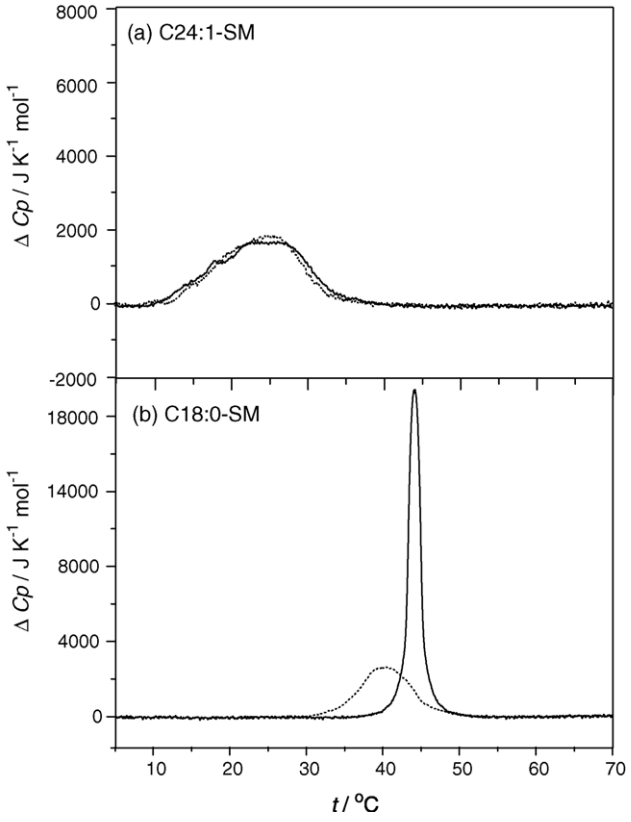

Fig. 6. Comparison of phase transition behavior between the sonicated and unsonicated vesicles for (a) the C18:0-SM and (b) the C24:1-SM. In this figure, the unsonicated vesicles are shown by solid lines and the sonicated vesicles are shown by dotted lines.

dimyristoylphosphatidylcholine (DMPC) [20] has reported that the phase transition behavior is clearly distinguished between the SUVs and MLVs, thus, the MLVs show a sharp, cooperative transition peak, in contrast to a broad peak for the sonicated SUVs caused by both a highly curved surface and a loosely packed chain. On this basis, the transition peak of the broad shape and the low transition temperature observed for the saturated C18:0-SM (Fig. 6(b)) suggests that the sonication produces the SUVs although there is no micrographs for this vesicles [15]. The present study reveals that the unsaturated C24:1-SM molecule spontaneously forms unilamellar vesicles in aqueous medium. This indicates that a thermodynamically stable form of the C24:1-SM molecule is the unilamellar vesicles. Accordingly, the unilamellar vesicle-forming property of the C24:1-SM would induce a decrease in the multiplicity of vesicles of the C16:0-SM and C18:0-SM, so that the broadening and temperature-lowering of the transition peaks of the saturated SMs are observed in the presence of the unsaturated SM, as shown in Fig. 3A and B.

Here, focusing on the unilamellar vesicle-forming property of the C24:1-SM discussed above, we refer to the past study reported by other workers [13]. In this study, it has been reported that sonicated vesicles of the C24:1-SM have the ability to keep a water-soluble solute incorporated into their inside, although sonicated vesicles of the SMs of C16:0, C18:0, C22:0, and C24:0 lack its ability. This result is in good agreement with that obtained by the present study, suggesting that the sonicated vesicles of these saturated SMs are present in either an unstable or a metastable state, in contrast with a stable state for the sonicated vesicle of the unsaturated C24:1-SM. Presumably, the unstable and/or metastable SUVs of these saturated SMs would be converted to the MLVs present in a stable state, so that the internal solute would be released outside during the conversion process.

Finally, we should discuss the reason why the C24:1-SM molecule has the unilamellar vesicle-forming property. In this connection, we have previously reported that acidic dimyristoylphosphatidylglycerol (DMPG) molecule spontaneously forms a SUV in aqueous medium because a negatively charged head group of this molecule occupies a fairly larger cross-sectional area compared with its two hydrocarbon chains [22]. Accordingly, the DMPG molecule of the reversed corn form is forced to assemble in the SUV characterized by a highly curved surface. However, this concept for the DMPG molecule could not be adopted for the C24:1-SM molecule which has a *cis* double bond at the C-15 position of the acyl chain, because for the C24:1-SM the cross-sectional area occupied by the two hydrocarbon chains is not so different as that occupied by the head group. Accordingly, we need to search for another reason to explain the unilamellar vesicle-forming property for the C24:1-SM. In this connection, we should consider interdigitated chain packings in an intrabilayer because there is a marked difference in length between the fatty acid chain (C = 24) and sphingosine chain (C = 18) of the C24:1-SM [10–16,23]. In fact, two types of interdigitation packings have been proposed for saturated C24:0-SM [11,12,15,16,23]. However, there is some question to directly apply the interdigitation packings of C24:0-SM to those of the C24:1-SM having the *cis* double bond. Accordingly, it is necessary to obtain a structural information concerning interdigitation packings of the unsaturated C24:1-SM, and so we will proceed to a study of X-ray diffraction.

Acknowledgements

This work is supported in part by Grants-in-Aid for General Scientific Research (15550133) from Ministry of Education, Science and Culture, Japan, 2003, and by “High-Tech Research Center” Project for Private Universities: matching fund subsidy from MEXT (Ministry of Education, Culture, Sports, Science and Technology), 2004.

References

[1] D. Marsh, CRC Handbook of Lipid Bilayers, CRC Press, Boca Raton, FL, 1990, pp. 3–4.
[2] A. Rietveld, K. Simons, Biochim. Biophys. Acta 1376 (1998) 467–479.
[3] E. Mombelli, R. Morris, W. Taylor, F. Fraternali, Biophys. J. 84 (2003) 1507–1517.

[4] C.M. Talbott, I. Vorobyov, D. Borchman, K.G. Taylor, D.B. DuPre, M.C. Yappert, Biochim. Biophys. Acta 1467 (2000) 326–337.
[5] R.F.M. de Almeida, A. Fedorav, M. Prieto, Biophys. J. 85 (2003) 2406–2416.
[6] W. Pruzanski, E. Stefanski, F.C. de Beer, M.C. de Beer, A. Ravandi, A. Kuksis, J. Lipid Res. 41 (2000) 1035–1047.
[7] J.L. Kerwin, A.R. Tuininga, L.H. Ericsson, J. Lipid Res. 35 (1994) 1102–1113.
[8] G.G. Shipley, L.S. Avecilla, D.M. Small, J. Lipid Res. 15 (1974) 124–131.
[9] W.I. Calhoun, G.G. Shipley, Biochim. Biophys. Acta 555 (1979) 411–436.
[10] Y. Barenholz, J. Suurkuusk, D. Mountcastle, T.E. Thompson, R.L. Biltonen, Biochemistry 15 (1976) 2441–2447.
[11] T.J. McIntosh, S.A. Simon, D. Needhan, C-H. Huang, Biochemistry 31 (1992) 2012–2020.
[12] M. Kodama, M. Abe, Y. Kawasaki, K. Hayashi, S. Ohira, H. Nozaki, C. Katagiri, K. Inoue, H. Takahashi, Thermochim. Acta 416 (2004) 105–111.
[13] R. Cohen, Y. Barenholz, S. Gatt, A. Dagan, Chem. Phys. Lipids 35 (1984) 371–384.
[14] P.K. Sripada, P.R. Maulik, J.A. Hamilton, G.G. Shipley, J. Lipid Res. 28 (1987) 710–718.
[15] P.R. Maulik, D. Atkinson, G.G. Shipley, Biophys. J. 50 (1986) 1071–1077.
[16] P.R. Maulik, G.G. Shipley, Biophys. J. 69 (1995) 1909–1916.
[17] P.R. Maulik, G.G. Shipley, Biochemistry 30 (1996) 8025–8034.
[18] P.R. Maulik, G.G. Shipley, Biophys. J. 70 (1996) 2256–2265.
[19] A.D. Bangham, M.M. Standish, J.W. Watkins, J. Mol. Biol. 13 (1965) 238–252.
[20] M. Kodama, T. Miyata, Y. Takaichi, Biochim. Biophys. Acta 1169 (1993) 90–97.
[21] G.V. Marinetti, J. Lipid Res. 3 (1962) 1–20.
[22] M. Kodama, H. Aoki, T. Miyata, Biophys. Chem. 79 (1999) 205–217.
[23] I.W. Levin, Biochemistry 24 (1985) 6282–6286.